Closed-loop control of flow-induced sound in a flow duct with downstream resonant cavities

Z. B. Lu, D. Halim,[a] and L. Cheng[b]
Department of Mechanical Engineering, The Hong Kong Polytechnic University, Hung Hom, Kowloon, Hong Kong Special Administrative Region

(Received 30 December 2011; revised 28 December 2012; accepted 11 January 2013)

A closed-loop-controlled surface perturbation technique was developed for controlling the flow-induced sound in a flow duct and acoustic resonance inside downstream cavities. The surface perturbation was created by piezo-ceramic THUNDER (THin layer composite UNimorph Driver and sEnsoR) actuators embedded underneath the surface of a test model with a semi-circular leading edge. A modified closed-loop control scheme based on the down-sampling theory was proposed and implemented due to the practical vibration characteristic limitation of THUNDER actuators. The optimally tuned control achieved a sound pressure reduction of 17.5 dB in the duct and 22.6 dB inside the cavity at the vortex shedding frequency, respectively. Changes brought up by the control in both flow and acoustic fields were analyzed in terms of the spectrum phase shift of the flow field over the upper surface of the test model, and a shift in the vortex shedding frequency. The physical mechanism behind the control was investigated in the view of developing an optimal control strategy. © *2013 Acoustical Society of America*. [http://dx.doi.org/10.1121/1.4789898]

PACS number(s): 43.50.Ki, 43.28.Py, 43.28.Ra [BSC] Pages: 1468–1479

I. INTRODUCTION

Vortex shedding behind a bluff body placed in a cross flow creates alternating lift and drag forces on the rear surface of the body.[1] This phenomenon can potentially cause serious structural vibrations of the bluff body and generate acoustic noise at the same time. The problem is accentuated when a downstream cavity exists and the shedding frequency coincides with the natural frequency of the cavity.[2,3] This phenomenon is generally referred to as flow-induced acoustic resonance which can be classified as one kind of flow-structure-sound (FSS) interaction problems. FSS is relevant to a large variety of applications in mechanical, civil, and environmental engineering, thus arousing extensive research interest over the last few decades.

FSS can be controlled by using either passive or active control methods.[4] Without requiring additional energy input, typical passive control methods include surface modifications with roughness, splitter plates, and small secondary control cylinders.[5–7] In active control methods, the flow system is altered via actuators which are driven by the external energy input. Active control methods can further be classified as open- and closed-loop control depending on whether feedback signals are used in the control process. Rotary, streamwise, transverse oscillations of a bluff body and inflow oscillation[8–11] are the representative open-loop control examples. However, the open-loop control performance is limited since the control signal is not directly related to the response of the system. This problem can be solved by using active closed-loop control, in which the input signal to the actuators is continuously adjusted based on the corresponding feedback signals acquired by sensors. Typical examples include Berger,[12] who introduced the single-sensor feedback control by actuating a bimorph cylinder with signals from a hot-wire sensor located in the wake. Huang and Weaver[13] used the fluctuating acoustic pressure inside the cavity as feedback signals, to drive the loudspeakers at the entrance of the tunnel. Cattafesta *et al.*[14–16] used an oscillating flap hinged near a cavity leading edge to disturb the shear layer separation, with feedback signals taken from the fluctuating acoustic pressure measured by a microphone within the cavity. Ziada *et al.*[17,18] studied the effect of feedback control on the excited acoustic resonance by using a synthetic jet to impart the control effect to the flow at the upstream edge of the cavity. These works, however, are mainly focused on the control of individual elements such as flow field, structural vibration, or acoustic noise. In fact, considering the coupling nature of the vortex-vibration-noise system, a simultaneous control targeting all these elements would probably be more effective.

Along this line of thinking, a surface perturbation technique was proposed by Cheng *et al.*,[19] aiming at the simultaneous control of both flow field and structural vibration. The technique makes use of curved piezo-ceramic actuators, embedded underneath the structural surface, to generate a controllable transverse motion on a structural surface for altering fluid-structure interactions. The effectiveness of this technique was experimentally assessed through a series of investigations in Zhang *et al.*[20–23] by using THUNDER (THin layer composite UNimorph Driver and sEnsoR) actuators.[24] It was demonstrated that the actively controlled perturbation could successfully alter the interactions by synchronizing the motion of the bluff body's upper surface and vortex shedding. Subsequently, both vortex shedding strength and the vortex-induced structural vibration could be simultaneously attenuated.

[a]Present address: Division of Engineering, The University of Nottingham, Ningbo, China.
[b]Author to whom correspondence should be addressed. Electronic mail: mmlcheng@polyu.edu.hk

The feasibility of using the proposed technique for the control of flow-induced acoustic resonance with downstream acoustic cavities was investigated by Zhang *et al.*[25] and more recently improved further by Lu *et al.*,[26] both using the open-loop control scheme. This later work provided a comprehensive assessment on the efficiency of the technique by using an improved actuator configuration, and more importantly, offered explanations on the control mechanism of the perturbation technique in attenuating the flow-induced sound. It was demonstrated that the effective reduction in the acoustic resonance is originated not only from a direct impairment of the vortex shedding strength, but also from the perturbation-induced vortex shedding frequency shift, that could be predicted using a simple formula,[26] which described that the shift was linearly related to the equivalent increase of the thickness of the bluff body in a flow duct.

As a continuation of the previous work, the control of flow-induced sound in a duct and the acoustic resonance inside downstream cavities was experimentally investigated using the closed-loop scheme in the present paper. Major objectives are twofold: (1) To establish a general closed-loop control strategy using the surface perturbation technique. Due to the practical vibration characteristic limitation of the THUNDER actuators, the feedback signals used in the closed-loop control were dealt with a special signal processing which was based on the down-sampling theory. (2) To assess the effectiveness of the control and provide additional evidence towards a better understanding of the underlying physics, and by the same token, an optimal control strategy can be proposed.

II. EXPERIMENTAL CONDITION

A closed circuit acoustic wind tunnel was used to conduct the present experiments.[25] It had an 1820-mm-long square test section of 100 mm × 100 mm. A parabolic contraction at the inlet was used to improve the uniformity of the flow velocity profile, and reduce the boundary layer thickness. A flat-walled diffuser at the downstream of the working section, with a half angle of 14°, was used to increase pressure recovery. The maximum flow velocity was 50 m/s with a turbulence intensity of less than 0.1% in the upstream section. Low background noise was achieved in this wind tunnel since noise of the motor and fan was mostly absorbed by acoustic duct linings.

A rigid thick plate with an angle of attack of zero, called the "test model" in the present experiment, was installed at 370 mm downstream of the exit plane of tunnel contraction in the flow duct. The two ends of the test model were rigidly fixed on the walls of the duct and served as vortex generator. At the downstream of the duct, two identical cavities with square cross sections were installed and they were symmetrical to the streamwise flow line. The test model and the cavity dimension, as well as the flow speed, were set so that acoustic resonance took place inside the cavities at the vortex shedding frequency.

THUNDER actuators were used in the present experiment for creating controllable perturbation on the upper surface of the test model. THUNDER, developed by NASA Langley research center, is a ferroelectric device made of multiple layers of material, typically stainless steel, aluminum, and PZT piezoceramic. Individual material layers are held together in a "sandwich-like" package using a NASA patented high temperature polyimide adhesive called LaRC™-SI. Compared to other conventional transducers, THUNDER can provide a large displacement (up to 2 mm) and a relatively large load capacity, smaller dimensions, with more reliability, strength, and flexibility. In particular, its larger displacement means that it can be used more effectively for generating a controlled surface perturbation than other conventional piezoelectric-based actuators with more limited displacements. Due to its special characteristics, it is most commonly used in actuators and acoustic sound generators. Its main drawback, however, is that its displacement behavior varies significantly with frequency. This is the reason why we propose the down-sampling control method in this work so that the THUNDER actuator can operate at its maximum displacement.

Details of the test model are shown in Fig. 1. It had a semi-circular leading edge and a height of $h = 11$ mm and a width of $w = 23$ mm. Two curved THUNDER piezo-ceramic actuators, with a length of 63 mm and a width of 14 mm, were embedded in a slot of 16 mm wide and 7 mm deep on the top side of vortex generator and 1.0 mm from the test model trailing edge. In order to create a maximum perturbation displacement in the transverse y-direction, the actuators were installed in a cantilever manner. A thin plastic plate of 1.2 mm thickness called a "vibration plate" was mounted flush with the upper surface of the plate, and connected with the cantilevered end of the THUNDER actuators by using double-sided tape. The vibration plate driven by the actuators would oscillate to create a span-wise uniform transverse vibration along the y-direction of the test model, which were confirmed by the measurement of velocity over the plate using a laser vibrometer.

Figure 2 shows the entire test configuration together with the measurement system. The depth (L) and width (B) of the two side cavities were chosen to be 487 mm and 70 mm, respectively. The distance between the trailing edge of the test model and the front edge of the cavity was 100 mm. Based on the test configuration, the first acoustic resonance frequency of the cavity (f_a') was estimated as

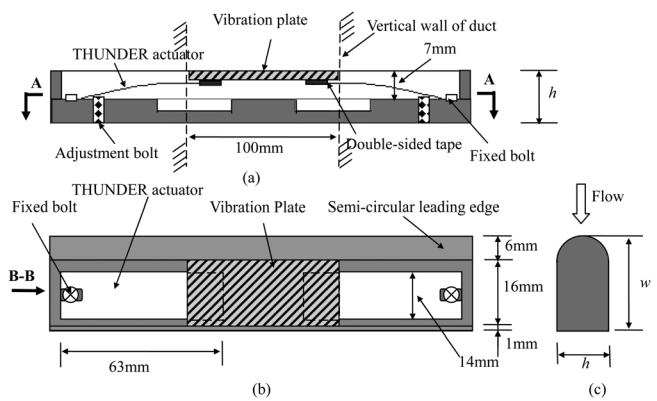

FIG. 1. Test model in details. (a) Installation, (b) top view A-A, (c) side view B-B.

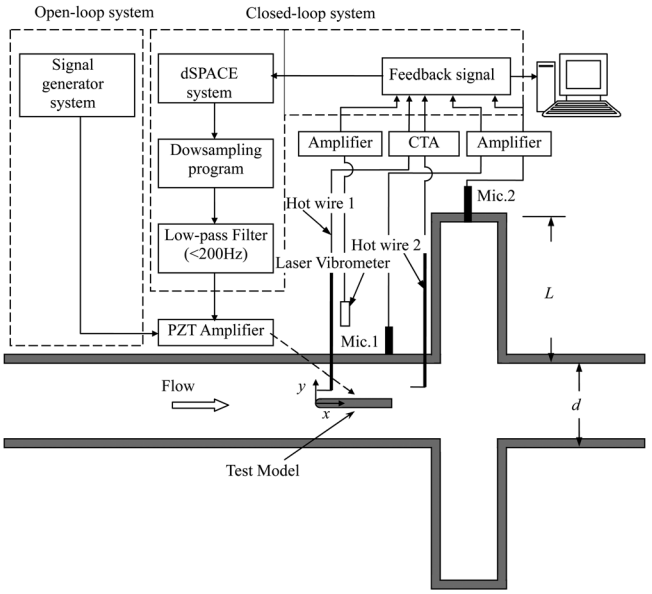

FIG. 2. Experimental setup, control system, and measurement system.

$f_a' = c/2(2L + d) \approx 159.5\,\text{Hz}$,[27] where c was the sound speed and d was the height of the duct. The corresponding critical flow velocity U_{cr} $(=f_s h/S_t)$ at resonance, when the shedding frequency was $f_s = f_a'$, was estimated to be about 8.2 m/s, using a Strouhal number St of 0.22, as suggested by Welsh *et al.*[28] for similar w/h ratios.

To generate the control perturbation, two cantilever actuators were simultaneously activated by a sinusoidal signal with controllable frequency, using the dSPACE rapid control prototyping system, and then amplified by a dual-channel PZT amplifier (Trek PZD 700), as shown in Fig. 2. The actuators were simultaneously activated in two different ways: (1) by a sinusoidal signal at a tunable frequency to form an open-loop control scheme and (2) by feedback signals acquired from system response to form a closed-loop control scheme. In the present work, the open-loop control scheme was used only for performance comparisons with respect to the closed-loop control scheme.

The acoustic pressures were measured by two 1/2 in. condenser microphones (B&K 4189). Microphone 1, referred to as Mic. 1 hereafter, was flush-mounted on the top wall of the duct at $x = 23$ mm. Another microphone, Mic. 2, was flush-mounted at the center of the top side-wall of the cavity. Two sets of 5 μm tungsten single hot wire were deployed to measure the fluctuating flow velocity at various positions around the test model. Hot wire 1 was fixed at the leading edge of test model at $x = 0$ mm and $y = 11$ mm, while hot wire 2 could be located at any positions around the test model depending on the requirement of the measurement. In addition, a Polytec Series 3000 Dual Beam laser vibrometer was used to measure the perturbation displacement produced by actuators. All measurement signals were recorded for the duration of 11 s using a personal computer through a 12-bit A/D board at a sampling frequency of 5890 Hz per channel after amplification.

The closed-loop control process is described in Fig. 2. In principle, the control can utilize any feedback signals acquired from the system, which may be from the hot wire 1, hot wire 2, Mic. 1, or Mic. 2. The feedback signal is then adjusted using the developed down-sampling algorithm implemented via dSPACE system, before being applied to the PZT amplifier. The detail of the down-sampling theory used for closed-loop control is described in Sec. III.

III. DOWN-SAMPLING THEORY AND ITS IMPLEMENTATION FOR REAL-TIME CLOSED-LOOP CONTROL

In a standard configuration, a closed-loop control system directly utilizes feedback signals that are acquired from sensors. A mainly tonal feedback signal can be amplified by a control gain, resulting in a closed-loop control actuation dominated by the primary tonal frequency of the feedback signal. However, in the current experimental set-up utilizing THUNDER actuators, it was found that there was a main difficulty in directly implementing such a control configuration due to the unique vibration response characteristic of the THUNDER actuators. To illustrate this, an observation was performed by setting the test model's control voltage to 160 V. The vibration characteristics of the test model, with embedded THUNDER actuators, were then measured by using a laser vibrometer at varying controlled excitation frequencies as shown in Fig. 3. It was observed that the test model's frequency response peaked at around 30 Hz, and rapidly decreased in magnitude as the excitation frequency increased. The displacement of control actuation of the test model was measured to be only 0.016 mm at the vortex shedding frequency of 160 Hz, compared to the maximum displacement of 0.900 mm at approximately 30 Hz. It is clear that such a small actuation of only 1.8% of the test model's maximum capability would be insufficient for achieving a satisfactory control performance. Therefore, to avoid such a control actuation problem, a down-sampling control method was proposed to bring down the frequency of the control actuation closer to the optimal operating frequency of the test model. In other words, feedback signals at approximately 160 Hz would be down-sampled to a much lower frequency of approximately 30 Hz, which is the optimal operating frequency of the test model.

A. Down-sampling of feedback signals for closed-loop control

Consider a feedback signal acquired from a sensor, containing information about the vortex shedding process. One can consider a typical original Fourier spectrum of the vortex

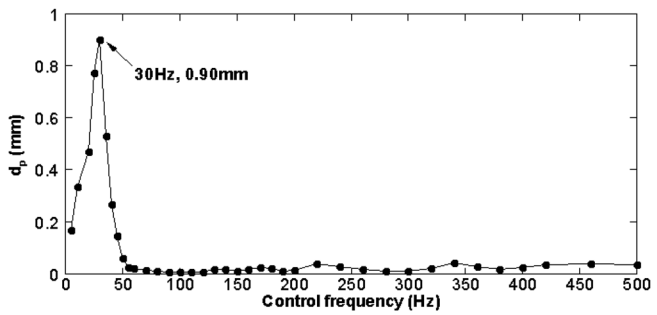

FIG. 3. Vibration characteristic of the test model at various control frequencies. The control voltage was set to 160 V.

shedding system $G_0(f)$ with its dominant response at and around the vortex shedding frequency $f_{\text{source}} = f_s$ as shown in Fig. 4. Since the feedback signal is real-valued, the spectrum is symmetric about zero frequency. Such a typical spectrum contains two dominant negative- and positive-frequency narrow-band spectra around the negative and positive vortex shedding frequencies, each with the frequency bandwidth of BF. In this case, the frequency bandwidth for both narrow-band spectra is $f \in [-f_{\text{source}} - BF/2, -f_{\text{source}} + BF/2] \cup [f_{\text{source}} - BF/2, f_{\text{source}} + BF/2]$. These narrow-band spectra contain most of the spectrum energy associated with the vortex shedding and flow-induced acoustic resonance processes. Thus, it is imperative that the down-sampling method should focus on "shifting" these narrow-band spectra to lower frequencies with minimal distortion for an effective control actuation of the test model.

It is known that as a consequence of sampling process, image spectra are generated from the original spectrum shifted by integer multiples of the sampling frequency f_{NS}.[29] In a standard sampling process according to the Nyquist–Shannon sampling theorem,[30] f_{NS} needs to be at least greater than twice the highest frequency of the band-limited continuous signal. This is to avoid the aliasing where the reconstructed sampled signal is distorted compared to the original signal measured by the sensors. However, the interest in this work is to generate the image narrow-band spectrum at low frequencies so that the reconstructed signal can be used as a feedback signal to drive the THUNDER actuator at its optimal operating frequency. To achieve this, a down-sampling method is utilized, using a sampling frequency lower than that recommended by the Nyquist–Shannon sampling theorem.

Let spectrum $G_n(f)$, with subscript n being a non-zero integer number, to be the image spectrum associated with n multiples of f_{NS}. As illustrated in Fig. 4, $G_1(f)$ is the image spectrum associated with $n \times f_{NS}(n = 1)$ in the positive f axis, while $G_{-1}(f)$ is the image spectrum associated with $n \times f_{NS}(n = -1)$ in the negative f axis. To simplify the illustration, only spectrum $G_0(f)$, $G_1(f)$, and $G_{-1}(f)$ are shown in Fig. 4, excluding spectrum with higher integer multiples of f_{NS}.

From Fig. 4, it is clear that the lower sampling frequency causes the image spectrum $G_1(f)$ and $G_{-1}(f)$ to overlap the original spectrum. The task now is how to choose an appropriate sampling frequency such that the narrow-band spectrum can be generated at lower frequencies. Since the narrow-band spectrum peak is located at the vortex shedding frequency f_{source}, the task is to "shift" this peak to the target frequency f_{target}, which is the THUNDER actuators' optimal operating frequency. Considering the original spectrum $G_0(f)$ and its positive-frequency image spectrum $G_1(f)$ in Fig. 4, the target frequency can be related to the vortex shedding and down-sampling frequencies as follows:

$$f_{\text{target}} = f_{\text{NS}} - f_{\text{source}}. \tag{1}$$

The significance of Eq. (1) is that since f_{source} is generally known based on the observation of vortex shedding process, one can choose a proper down-sampling frequency f_{NS} correspondingly to "shift" the narrow-band spectrum to a lower target frequency. As the result, two low-frequency narrow-band image spectra centered at $-f_{\text{target}}$ and f_{target} can be generated as depicted in Fig. 4.

However, although the narrow-band image spectra have been shifted to lower frequencies, a problem still needs to be resolved. Due to the down-sampling process, overlapping image spectra associated with integer multiples of the sampling frequency f_{NS}, can in fact distort the overall spectrum, leading to a distorted reconstructed signal with multiple tonal components. To avoid such a distortion, a band-pass filter with the pass-band frequency of $f \in [f_{\text{target}} - BF/2, f_{\text{target}} + BF/2]$ is utilized to reject the off-bandwidth spectrum contributions as shown in Fig. 4. This way, the narrow-band image spectrum located at and nearby the target frequency will be the only primary spectrum to be reconstructed. It should be appropriate to comment here that although multiple narrow-band spectra would be generated at integer multiples of down-sampling frequency, their spectrum contributions within the pass-band frequency BF, centered at f_{target}, are minimal because of their narrow-band spectrum characteristics. Finally, the down-sampled image spectrum can be reconstructed to obtain the low-frequency continuous signal that is needed for effective control actuation using the test model.

The argument proposed in using this down-sampling strategy is as follows. This work considers the typical situation where there is a gradual change in system dynamics. Due to a lower control actuation frequency, there is a control delay to be expected in responding to changes in vortex shedding behavior. Since the changes in system dynamics are gradual, the control actuation will have sufficient time to response to the vortex shedding changes as will be demonstrated in the experiments. In other words, changes in vortex shedding behavior will be detected after several vortex shedding cycles and the control actuation will then be performed to respond to the changes to modify the flow field via surface perturbation.

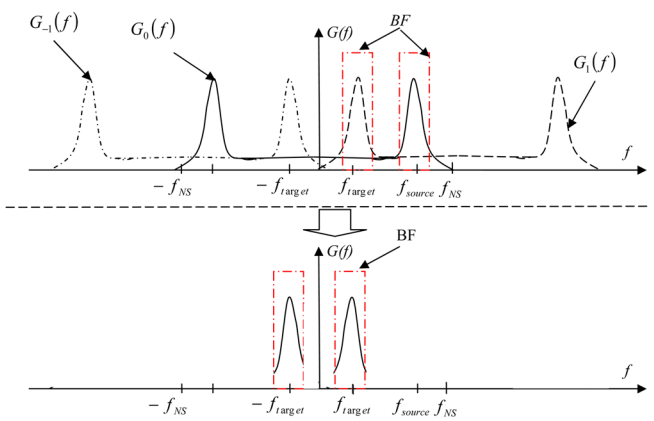

FIG. 4. (Color online) Schematic of the down-sampling process.

B. Implementation of down-sampling method for real-time control of flow-induced acoustic resonance

Based on the developed down-sampling method, a real-time closed-loop control experiment was undertaken. The

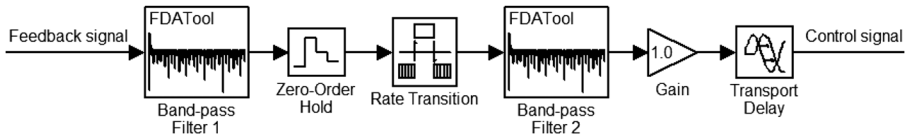

FIG. 5. Down-sampling algorithm for closed-loop control.

closed-loop control was aimed to impair the vortex shedding process, whose shedding frequency was at approximately 160 Hz, by using the surface perturbation of the test model. The optimal operating frequency of the test model was approximately 30 Hz, so the target frequency was set to 30 Hz. As mentioned in Sec. II, the original sampling frequency of 5890 Hz was used in the experiment. Furthermore, for the simplicity of down-sampling implementation, the down-sampling frequency f_{NS} was chosen to be an integer multiple of the original sampling frequency. Based on these control criteria, the down-sampling frequency f_{NS} was determined to be 190 Hz from Eq. (1).

A real-time down-sampling control system was implemented via dSPACE/Simulink system as shown in Fig. 5. The control modules could be described as follows. (1) A band-pass filter with a pass-band frequency from 150 to 170 Hz, called the "Band-pass filter 1," was used to capture components of feedback signal that contain most of the vortex shedding energy. (2) A zero-order hold module was then used to down-sample the sampling frequency of the signal from 5890 to 190 Hz. To be precise, it was used to down-sample the original signal to a lower-frequency signal by holding the signal value fixed over a multiple-sample interval at the time step of $\Delta t = 0.00526$ s, which corresponds to the down-sampling frequency f_{NS} of 190 Hz. (3) A rate transition module was used to update the sampling time step from the original $\Delta t = 0.00017$ s to the down-sampled time step of $\Delta t = 0.00526$ s. (4) An arrow band-pass filter with a pass-band frequency from 29 to 31 Hz, called "Band-pass filter 2," was utilized to reject the off-bandwidth image spectrum. (5) Finally, the gain and transport delay modules were, respectively, used to adjust the magnitude A and phase delay ϕ of the down-sampled signal for closed-loop control, which will be explained in the following section.

IV. INVESTIGATION INTO OPTIMAL CONTROL PARAMETERS AND CONTROL PERFORMANCE

A. Flow structure and flow-induced resonance

In the current configuration, a semi-circular leading edge test model is placed in a duct with uniform incoming flow at a moderate flow velocity; the boundary layer separates at the trailing edge and the vortex shedding, called the "trailing edge vortex shedding," is formed by the interaction of shear layers after the trailing edge.[28] It should be noted that the present configuration does not resemble the locked-in acoustic resonance case as discussed in Ziada's research.[17,18] In this work, the acoustic resonance is induced by the vortex shedding generated downstream of a test model in a flow duct. There only exists a small degree of feedback from the acoustic resonance to the vortex shedding process, which causes an additional control challenge that is the main focus of this work.

The effect on downstream cavity resonance was investigated by using the sound pressure level (SPL) spectra measured by the two microphones. The results are shown as Fig. 6 in terms of $\Delta\text{SPL} = \text{SPL}_{m2} - \text{SPL}_{m1}$, with SPL_{m2} and SPL_{m1} being the sound pressure levels at Mic. 2 and Mic. 1, respectively. Sound pressure level inside the cavity was obviously higher than that in the duct around the region of cavity resonance frequency f_a', implying that the sound was amplified by the cavity resonance effect. Furthermore, a series of tests were conducted to document the sound pressure level measured by Mic. 1 and Mic. 2 at shedding frequency f_s under various flow velocities without any control action, for determining the resonance bandwidth. The results are shown in Fig. 7. The peak values of sound pressure level at f_s measured by Mic. 2, reached a peak value of 97.8 dB when the free-stream velocity $U_\infty = U_{cr} = 8.2$ m/s (i.e., $f_s = f_a' = 159.5$ Hz). Using the conventional definition of the bandwidth corresponding to 3 dB reduction compared to the peak value, the bandwidth of the resonance peak was determined as 3.3 Hz from 158.3 to 161.6 Hz, corresponding to a flow velocity variation from 8.0 to 8.3 m/s. Therefore, at a moderate flow velocity and particular depths of the cavities, a strong flow-induced acoustic resonance inside downstream cavities can be excited by the trailing edge vortex shedding from the test model. Such a configuration was used in this work to demonstrate the performance of our proposed control strategy to minimize the acoustic resonance within the cavities.

B. The optimal control voltage and phase delay

The developed closed-loop control system was implemented to the system to control the flow-induced sound in the duct and the acoustic resonance in the cavity. There are two primary control parameters that govern how the control actuation was applied to the system: the gain and phase delay relative to the down-sampled feedback signal. Investigation was undertaken to study the impact of these control parameters to the controller ability to regulate the flow and sound fields. For this purpose, direct feedback control was

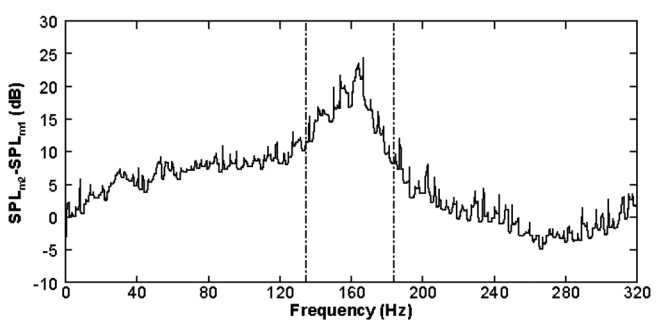

FIG. 6. Downstream cavity resonance, $L = 487$ mm, $d = 100$ mm, $U_\infty = 8.2$ m/s.

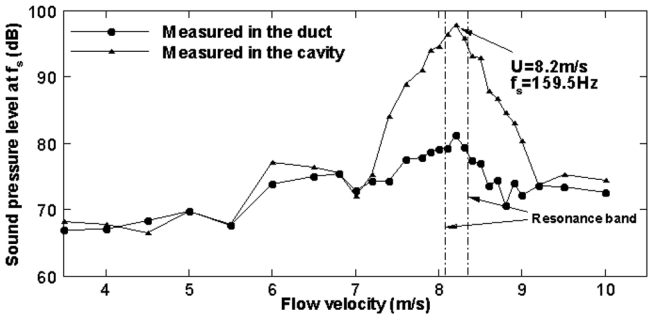

FIG. 7. Sound pressure level at f_s for various flow velocities without control.

implemented with two tunable control parameters, the magnitude A and phase delay ϕ, that can be systematically adjusted for performance analysis, as well as for identifying the optimal control parameters.

Initially, closed-loop control using multiple feedback signals from the hot wire 1, hot wire 2, Mic. 1, and Mic. 2 was investigated. Various measurements were conducted to check the control performance obtained by using the combination of feedback signals. However, it was found that no obvious improvement was obtained by using multiple feedback signals, compared to using a single feedback signal from hot wire 2. One plausible reason is that all signals contained the same information of the mainly tonal vortex shedding response in the flow or sound fields. Furthermore, microphones could be affected by the background acoustic noise that could negate the advantage of having multiple feedback signals for control. Thus in this work, it was decided that the closed-loop control was to be implemented by using a single feedback signal from hot wire 2.

The effects of control magnitude and phase delay on the control performance were investigated. The optimal control voltage was searched by varying the magnitude of down-sampled feedback signal to generate voltage V_p for the control actuation of the test model. The effect of varying the control voltage, while the phase delay was kept at $\phi = 0$, on the noise reduction of flow-induced acoustic resonance in the cavity is shown in Fig. 8 in terms of sound pressure level reduction (ΔSPL). This section focuses on the closed-loop control results, while their comparisons with those of open-loop control, as shown in Fig. 8, are to be discussed in detail in Sec. V. The control voltage limited by the maximum voltage allowable for THUNDER actuators was about 160 V. As expected, the control performance at low control voltages was minimal, which justified the need to use the proposed down-sampling control method to optimize the control actuation of the test model. Furthermore, microphones in the duct and cavity both recorded the same general trend of increasing noise reduction as the control voltage was increased. For the present case, the best control result was obtained when the control voltage $V_p = 155$ V, resulting in a SPL reduction of 17.1 dB in the duct and 21.5 dB inside the cavity, respectively.

Figure 9 shows the control performance when the phase delay relative to the feedback signal was varied, while the control voltage was fixed at $V_p = 155$ V. The general trends of noise reduction measured by microphones in the cavity and duct were similar, indicating a consistent physical mechanism occurred in the system. The best control performance occurred when the control phase delay was at approximately 288°, with the obtained noise reduction of 17.5 dB in the duct and 22.6 dB inside the cavity at the vortex shedding frequency. The results thus indicate the existence of the optimal control phase delay, which allows for an efficient closed-loop noise control inside the cavity and in the duct.

C. The closed-loop control performance in the sound and flow fields

Using the optimal control voltage and phase delay, the closed-loop control performance was investigated in both sound and flow fields. Figures 10(a) and 10(b) depict the sound pressure spectra obtained from the fast Fourier transform of time domain signals from respective Mic. 1 and Mic. 2 measurements, with a frequency resolution of 0.1 Hz. It can be seen that, upon deployment of the control, the sound pressures in the duct and inside the cavity underwent significant reductions. The spectra indicated that with control, the SPL in the duct decreased from 81.3 to 63.8 dB (a reduction of 17.5 dB) at the vortex shedding frequency. Meanwhile, the SPL measured inside the cavity decreased from 97.8 to 75.1 dB (a reduction of 22.6 dB), which was much larger than the noise reduction measured in the duct. Such a phenomenon will be discussed in details in Sec. V. The experimental results demonstrated that the closed-loop control in the sound field was indeed effective. Furthermore, it was found that there was a moderate increase in noise level at low frequencies when control was applied on the system,

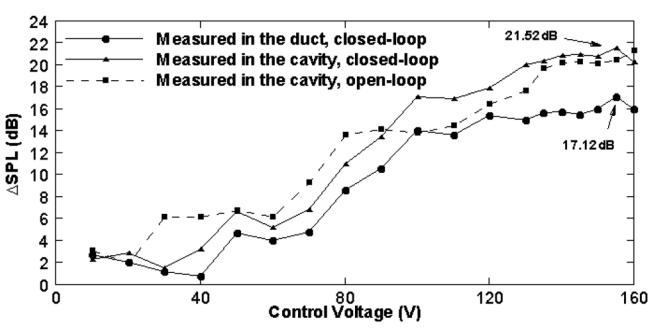

FIG. 8. Control effect for different control voltages. The control signal was from hot wire 2 which was located at $x = 35.5$ mm, $y = 11$ mm.

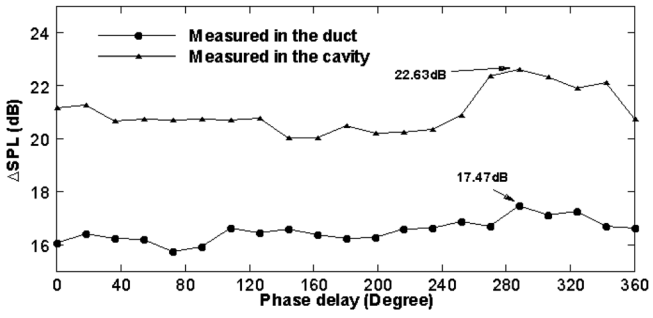

FIG. 9. Closed-loop control performance for varying control phase delays. The feedback signal was obtained from the hot wire 2 located at $x = 35.5$ mm, $y = 11$ mm and the control voltage was 155 V.

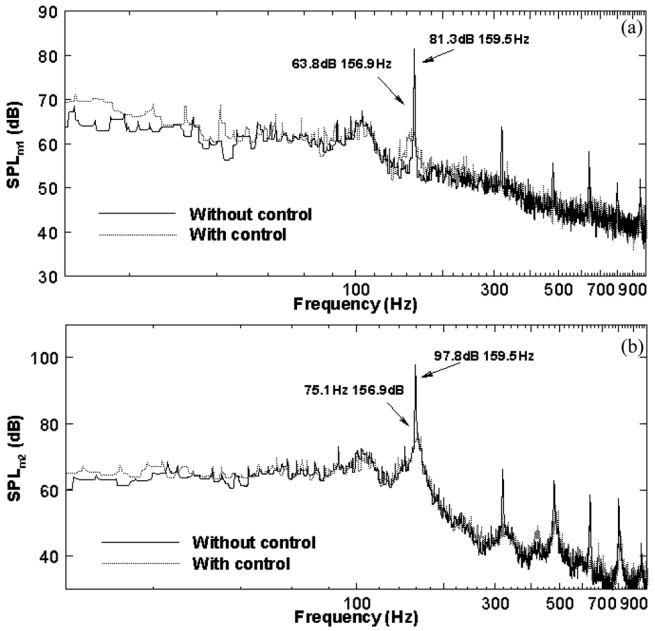

FIG. 10. Closed-loop control performance shown in frequency-domain. (a) Measured in the duct; (b) measured inside the cavity.

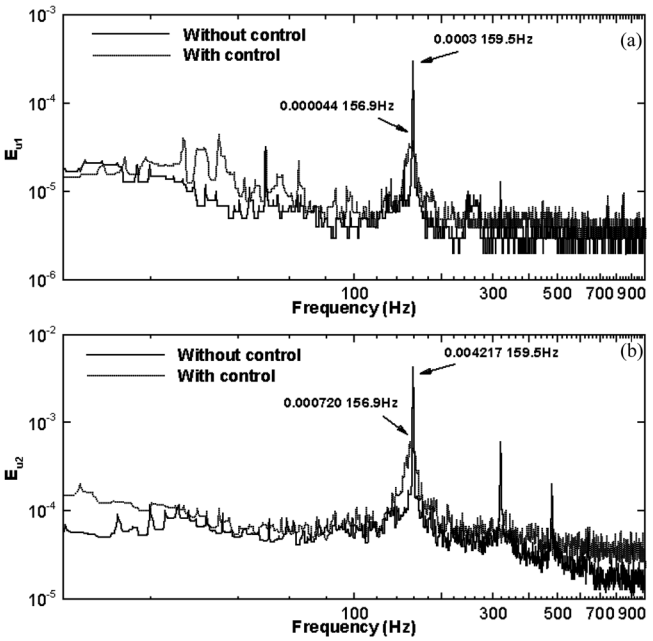

FIG. 11. Closed-loop control performance shown in frequency-domain. (a) Measured by hot wire 1 at $x = 0$ mm, $y = 11$ mm; (b) Measured by hot wire 2 at $x = 34$ mm; $y = 11$ mm.

as shown in Figs. 10(a) and 10(b). This extra noise was generated by the fluid-structure interaction between the upper surface of the vibration plate and the flow field around the test model at the optimal control frequency. In the cavity, however, the low-frequency SPL was still considerably lower than the primary noise SPL at the vortex shedding frequency, which means the extra noise would not significantly impact on the overall noise control efficiency. The experimental results demonstrated that the closed-loop control in the sound field at the vortex shedding frequency was indeed effective.

The effect of closed-loop control in the flow field was investigated in terms of the power spectrum density of flow velocity E_u measured by two hot wires, located at the leading edge (hot wire 1) with $x = 0$ mm, $y = 11$ mm and at downstream of the test model (hot wire 2) with $x = 34$ mm, $y = 11$ mm, as shown in Figs. 11(a) and 11(b). From the figures, it can be seen that E_u at the vortex shedding frequency has decreased from $3.1\,e{-}4$ to $4.4\,e{-}5$ (a reduction of about 86%) measured by hot wire 1 and $4.2\,e{-}3$ to $7.2\,e{-}4$ (a reduction of about 83%) measured by hot wire 2. Therefore, the closed-loop control in the flow field was also effective in reducing the flow velocity levels generated by the vortex shedding.

The corresponding control performances in time-domain were shown in Figs. 12 and 13. The signals were filtered by a 5-Hz band-pass filter centered at the vortex shedding frequency f_s. Upon deployment of the closed-loop control, the noise and flow velocity reductions were clearly observed in all four hot wire and microphone sensors, indicating that the vortex shedding was successfully impaired by the control action. These results demonstrate that the proposed closed-loop control using the down-sampling method can effectively alter the sound and flow fields generated by the vortex shedding with a desirable consequence of noise reduction inside the cavity.

V. DISCUSSION ON THE CONTROLMECHANISM

A. Fluid-structure alteration and fluid-sound interaction

Having demonstrated the effectiveness of the developed closed-loop control, it is important to further investigate its control mechanism in relation to the fluid-structure alteration around the test model and the fluid-sound interaction in the duct and cavities. This is done in the view of determining the optimal control configuration. To that end, the spectral coherence analysis was used to investigate the changes in fluid-structure alteration and fluid-sound interaction based on experimental measurements from microphone and hot wire sensors, respectively. The spectral coherence and spectral phase between two signals u_a and u_b can be calculated by[25]

$$\mathrm{coh}_{u_a u_b} = \frac{Co^2_{u_a u_b} + Q^2_{u_a u_b}}{E_{u_a} E_{u_b}}, \tag{2}$$

$$\phi_{u_a u_b} = \tan^{-1}\left(\frac{Q_{u_a u_b}}{Co_{u_a u_b}}\right), \tag{3}$$

where $Co_{u_a u_b}$ and $Q_{u_a u_b}$ are the co-spectrum and quadrature spectrum of signal u_a and signal u_b, respectively. The cross-spectrum was computed from the fast Fourier transform of the correlation $\overline{u_a(t+\tau)u_b(t)}$, where τ is the time delay. Here, E_{u_a} and E_{u_b} are the respective energy of the signals u_a and u_b. In the investigation, the optimal control configuration was used with the control voltage of 155 V and the phase delay of 288°.

First, the spectral coherence between the respective signals measured by hot wire 1 at $x = 0$ mm, $y = 11$ mm and hot wire 2, at $x = 34$ mm, $y = 11$ mm, is shown in Fig. 14. It

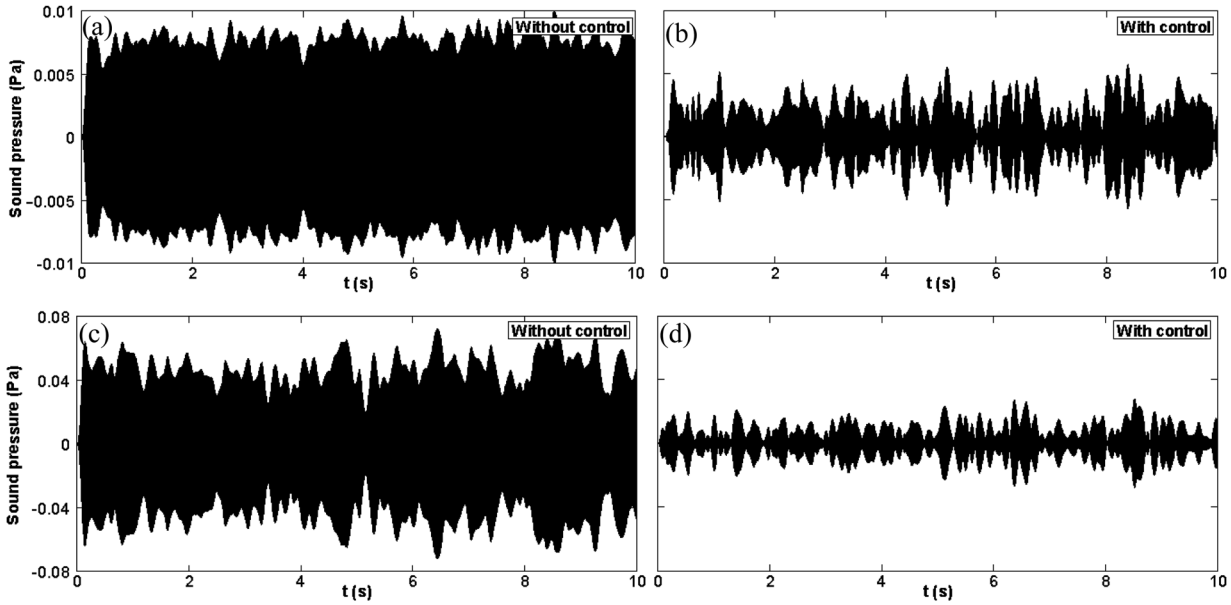

FIG. 12. Control performance in sound field shown in time-domain. Signals were filtered by a 5 Hz band-pass filter. (a) Without control, measured in the duct; (b) with control, measured in the duct; (c) without control, measured inside the cavity; (d) with control, measured inside the cavity.

was observed that the spectrum coherence at the vortex shedding frequency decreased from 0.475 to 0.215 (a reduction of about 54.7%). The reduction in the spectral coherence at the vortex shedding frequency indicated that the control action of the closed-loop control had actually impaired the vortex shedding at the downstream of the test model. Meanwhile, an increase in the spectral phase was also noticed (not shown here), suggesting that the vortex shedding had been slowed down by the control action,[25] which is agreeable with the vortex shedding frequency shift phenomena observed in the previous study.[26]

Based on the above observation, a mechanism for the fluid-structure alteration in the duct can be proposed. The control action applied on the upper surface of the test model generated the flow perturbation that interacted with the vortex shedding process to alter the generation of the trailing edge vortex shedding. Furthermore, the perturbed flow from the oscillating plate of the test model decreased the spatial coherence of the trailing edge vortex which was used to quantify the change in the flow structure in the present system. As shown in Fig. 14, when control was applied, the spectrum coherence at the vortex shedding frequency has changed, which indicates that the flow structure has changed due to the applied surface perturbation. This change resulted in the reduction of the trailing edge vortex shedding strength. Overall, the small local perturbation applied in the present system could alter the flow structure around the surface of the test model, which further disturbed the entrainment of

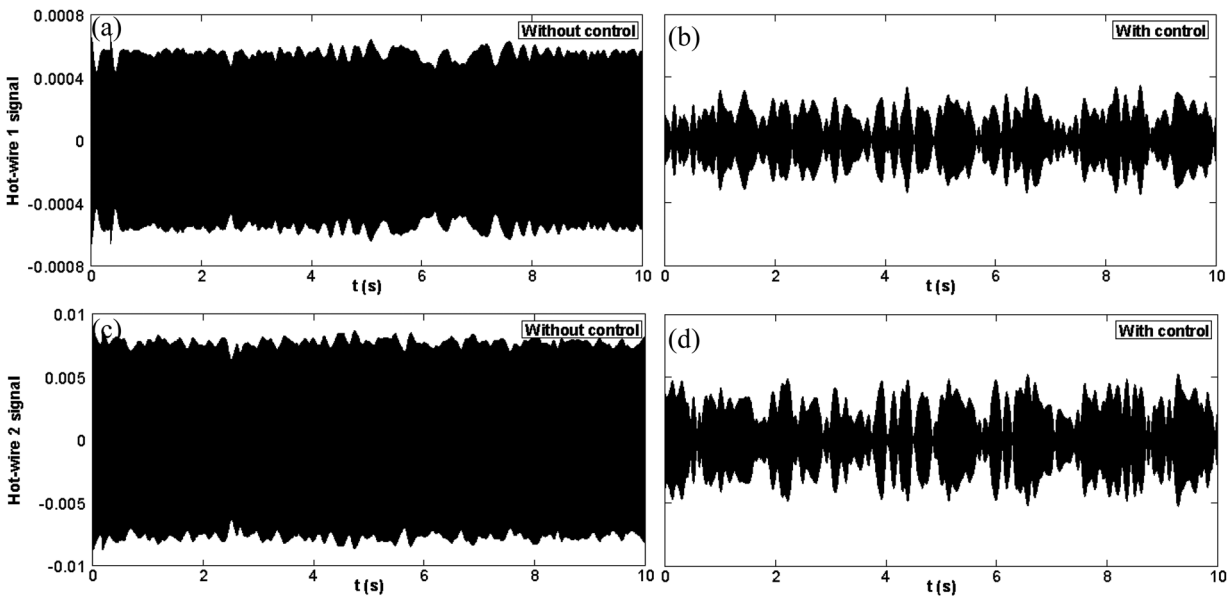

FIG. 13. Control performance in flow field shown in time-domain. (a) Without control, measured by hot wire 1; (b) with control, measured by hot wire 1; (c) without control, measured by hot wire 2; (d) with control, measured by hot wire 2.

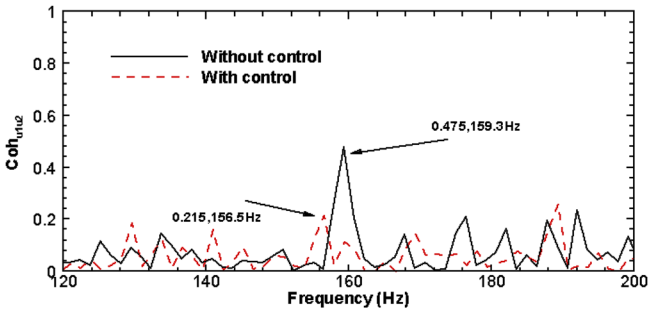

FIG. 14. (Color online) Spectral coherence at the vortex shedding frequency between u_1 and u_2 for closed-loop control.

the leading edge boundary layer to the trailing edge, leading to a reduction of the vortex strength in the duct.

Next, the fluid-sound interaction between the flow field in the duct and the acoustic resonance in the cavities was investigated. The spectral coherence between the respective signals measured by Mic. 2 in the cavity and hot wire 2 downstream the test model, at $x = 34$ mm, $y = 11$ mm, is shown in Fig. 15. It was observed that the spectrum coherence at the vortex shedding frequency decreased from 0.974 to 0.529 (a reduction of about 46%). The reduction in the spectral coherence at the vortex shedding frequency indicated that the control action had actually influenced the sound-field inside the cavities; the coherent fluid-sound interaction in the system has been impaired by the closed-loop control action, leading to a strength reduction in the flow-induced acoustic resonance phenomena inside the cavity as measured by Mic. 2. At the same time, the peak of the coherence was shifted to a low frequency value which means the vortex shedding frequency was shifted under the control action.

The physical mechanism can be explained in more details as follows. A flow-induced acoustic resonance inside downstream cavities was excited by the trailing edge vortex shedding from the test model. The small local perturbation applied on the upper surface of the test model modified the flow structure over the test model during control. This resulted in a change of the vortex shedding frequency, leading to an extra reduction of the resonances inside the cavities. The vortex shedding frequency shift was quantified in terms of perturbation displacement of test model. The advantage of using this approach is that one could directly relate such a displacement to the imposed surface perturbation. It was

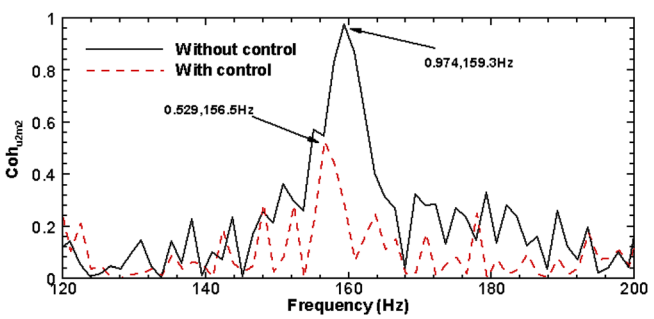

FIG. 15. (Color online) Spectral coherence at vortex shedding frequency between m_2 and u_2 for closed-loop control.

observed that the effect of perturbation could actually be related to an equivalent increase in the thickness of the test model, as shown in Fig. 17. Further details have been described in a previous study.[26] Based on those analyses, a possible explanation for the equivalent increase in the thickness of test model is due to the boundary-layer thickening, resulting in a shift in the vortex shedding frequency. Upon perturbation, the flow velocity generated by the vibration plate around the test model might alter the thickness of the boundary layer around the test model, resulting in an increase in the distance between the two shear layers, as observed as an equivalent increase in the overall thickness of the test model seen in Fig. 17.

In summary, the reduction of vortex shedding and flow-induced noise in the duct is mainly due to the impairment of the vortex strength upon deployment of control by altering the flow structure around the surface of the test model. Furthermore, the local surface perturbation brings about a shift, albeit slight, in the vortex shedding frequency that may result in an off-set of the acoustic resonance beyond its resonance bandwidth, especially for a lightly damped acoustic cavity. This phenomenon alone results in an additional sound reduction inside the cavities, as evidenced by the higher sound reduction inside the cavities as compared to that obtained in the duct.

B. Investigation on the spectral phase changes under control

Further investigation was done on the level of performance improvement that can be achieved by closed-loop control, relative to that of open-loop control. In this case, experiments on the open-loop control of the flow-induced acoustic resonance was conducted, whose control configuration has been discussed in detail in a previous work.[24] Figure 8 shows the level of sound reduction in the cavity when open-loop control was implemented. It can be observed that the open-loop and closed-loop control shared the same trend of sound reduction, although the closed-loop control could achieve a larger SPL reduction. One plausible explanation is that there are two different contributions on the control performance, one is the impairment of the vortex strength and the other one is the shedding frequency shift. The shedding frequency shift was observed to be dominant at higher control voltage, leading to a smaller performance difference between the open-loop and closed-loop control schemes at the best control performance. However, in a more general case for a moderate control voltage, a larger performance difference of up to 4 dB was observed. Such results were expected because the open-loop control actuation was independent of what was occurring in the system, while the closed-loop control actuation was directly influenced by the system response as reflected by the feedback signal. Therefore, the closed-loop control scheme could provide a more effective surface perturbation generated by the test model for disturbing generated vortices, leading to weaker vortex shedding and acoustic resonance inside the cavity.

To study the physical mechanisms of the vortex shedding process over the test model more thoroughly, the

spectral phase relationship between two measured flow velocities along the upper surface of the test model, u_1 and u_2, was analyzed. Here, u_1 was measured by hot wire 1 which was located at leading edge with $x = 0$ mm, $y = 11$ mm, while u_2 was measured by hot wire 2 which was moved along the line of $y = 11$ mm so the vortex shedding characteristic over the test model could be investigated.

Figure 16 shows the spectral phase at the vortex shedding frequency for three different cases: without control, with open-loop control, and with closed-loop control. The results showed that when there was no control actuation, each cycle of vortex shedding began at the trailing edge of the test model. Between the leading edge and trailing edge, there was no clear vortex shedding as indicated by no significant spectral phase shift over this region. In this case, the flow over the leading edge and trailing edge was rather in-phase. The spectral phase for the region $0 \leq x \leq 5.5$ mm was relatively small, however, the spectral phase shift began to increase significantly for the region $x > 5.5$ mm. Such a spectral phase shift indicated that the flow structure over this region had started to change, leading to a full generation of vortex shedding at the trailing edge.

Under the surface perturbation in the region 5.5 mm $< x <$ 23.0 mm over the test model, there was generally no vortex shedding that dominated within this range. Instead, the boundary layer dominated the flow field in this region. The irregularity of measured spectral phase shift reflected the complexity of the developed boundary layer over the test model. However, at the trailing edge of the test model, vortex shedding was fully developed and propagated downstream. From Fig. 16, a clear trend of monotonically decreasing spectral phase shift was observed. In the majority of regions downstream the test model, the value of the spectral phase shift for controlled system was larger than that of the uncontrolled system. The increase of the spectral phase shift value might imply that more time was required for a vortex to travel from the trailing edge to the downstream of the flow duct. This is consistent with the frequency shift phenomenon[24] where the vortex shedding frequency was slightly shifted to a lower frequency after control.

Further observation indicates that there was a generally larger spectral phase shift for systems with closed-loop control than those with open-loop control, as can be seen in Fig. 16. The result suggests that for closed-loop control, the active surface perturbation has generated a more significant change to the vortex shedding structure than that of open-loop control. Based on this investigation, an optimal control strategy using the developed control technique could be proposed by optimally tuning the phase-delay term of the control actuation to create effective changes in vortex shedding structure, as observed by the spectral phase shift in the flow field.

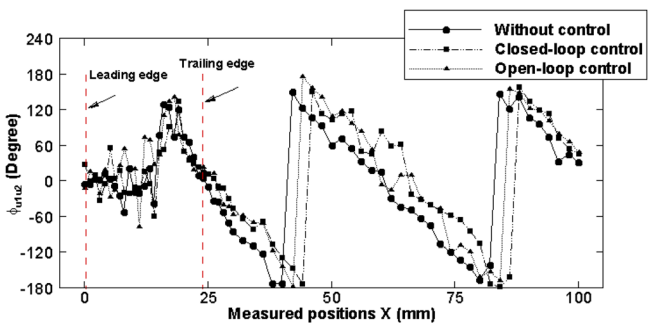

FIG. 16. (Color online) Spectral phase between u_1 and u_2 at the vortex shedding frequency along the x-direction. Here, u_1 was measured by hot-wire 1 which was located at $x = 0$ mm, $y = 11$ mm, while u_2 was measured by hot-wire 2 which was moved along the x-direction at fixed $y = 11$ mm.

C. Vortex shedding frequency shift in the closed-loop control

Previous work in open-loop control of flow-induced acoustic resonance[26] has observed the vortex shedding frequency shift phenomena, where the shedding frequency is shifted to a lower value under the control action. This frequency shift allows a larger level of noise reduction inside the cavity than in the duct because of the slight mismatch between the vortex shedding and the acoustic resonance frequencies of the downstream cavities, especially when the latter is lightly damped. The reduction of the vortex shedding frequency could be attributed to the effect of surface perturbation of test model, which could be regarded as a way to increase the effective thickness of test model. Interestingly, in the closed-loop control experiment, this phenomenon was also observed. To study this phenomenon, further investigation was done by quantifying the change in frequency shift to the maximum effective thickness of test model based on the closed-loop control scheme. It was found that the vortex shedding frequency shift can be predicted by an equation which relates the frequency shift to the maximum effective thickness of test model, and consequently to the control voltage actuation. Therefore, the same physical mechanism exists on this frequency shift phenomenon due to surface perturbation of the test model, independent of the control schemes. It had concluded that the vortex frequency shift could be expressed as[26]

$$\Delta f_{sp} = f_{s0} - f_{sp} = \frac{\bar{d}_p}{h} f_{s0}, \tag{4}$$

where Δf_{sp} is the change of the vortex shedding frequency, f_{s0} is the unperturbed vortex shedding frequency, f_{sp} is the perturbed vortex shedding frequency, h is the thickness of the test model, and $\bar{d}_p$ is the equivalent increase of the maximum thickness due to the control.

Equation (4) indicates that the reduction Δf_{sp} is linearly related to effective displacement $\bar{d}_p$. Based on Eq. (4), the variation of effective displacement $\bar{d}_p$ versus maximum displacement d_p measured by a laser vibrometer is shown in Fig. 17. Note that when $d_p > 0.75$ mm, there was an observable increase in the effective displacement $\bar{d}_p$. One plausible explanation is due to the nonlinear behavior of the fluid-structure interaction at a larger level of flow perturbation, leading to a desirable increase of vortex shedding frequency shift. This behavior might also explain that at higher control voltage of more than 140 V, the control performances for the open-loop and closed-loop control schemes were not significantly different as shown in Fig. 8.

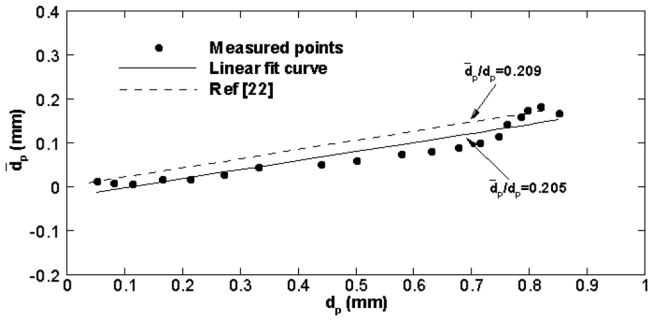

FIG. 17. Effective perturbation displacement of the vibration plate.

In this work, however, a linear representation was used to relate parameters $\bar{d}_p$ and d_p for simplicity. The relationship between the two parameters can be best approximated using a linear regression fitting line with a gradient $\bar{d}_p/d_p = 0.205$. The determined gradient for closed-loop control was in fact relatively similar to that for open-loop control of 0.209.[26] Comparing two fitting lines for both open- and closed-loop control in Fig. 17, it can be observed that the lines are reasonably close to each other, considering uncertainties that normally arise for these particular experimental measurements. The results confirm that the vortex shedding frequency shift phenomenon occurs mainly due to the surface modification of the test model, regardless of the control scheme used. The frequency shift can be predicted in a reasonably accurate way using a simple formula in Eq. (4).

Finally, in order to quantify the impact of this frequency shift on the noise reduction inside the cavity, measurements were conducted to document the noise control performance for control-on and control-off cases, measured at vortex shedding frequency f_s, at varying flow velocity from 3.5 up to 10 m/s. Note that the acoustic resonance occurred only when the flow velocity was set to 8.2 m/s. The control voltage input into the THUNDER actuators was fixed at its optimal level of $V_p = 155$ V and its optimal phase delay of $\phi = 288°$. The results are shown in Fig. 18, in terms of $\Delta\text{SPL} = \text{SPL}_{m2} - \text{SPL}_{m1}$, where SPL_{m2} and SPL_{m1} are the sound pressure levels at Mic. 2 and Mic. 1, respectively. It can be seen that apart from the resonance region, noise reductions in the duct and in the cavity are almost the same. This should be attributed to the weakened vortex strength. Around the cavity resonance, however, the noise reduction inside the cavity exceeds that in the duct, by as much as about 5.1 dB. This can be attributed to the control-induced shift of the vortex shedding

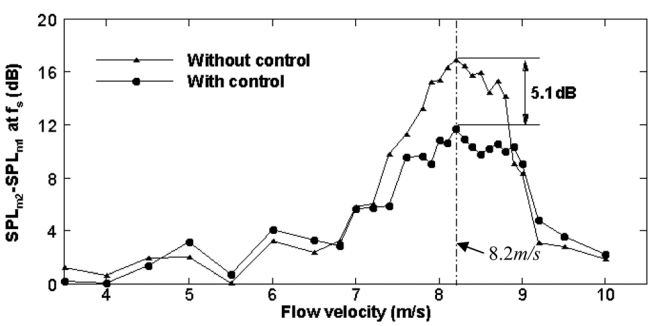

FIG. 18. Control effect on $\text{SPL}_{m2} - \text{SPL}_{m1}$ at f_s for various flow velocities.

frequency. In fact, a 2.6 Hz shift in f_s exceeds the half bandwidth of the cavity resonance.[24] This alone should bring about more than 3 dB reduction in the SPL.

In summary, the closed-loop control not only disturbs the shear layers behind the test model to weaken the vortex shedding strength, but also shifts the vortex shedding frequency, which further suppresses the acoustic resonance inside down-stream cavities. It is relevant to note that the present work was focused on a fixed moderate flow velocity. However, the proposed control strategy can simply be extended to other cases when the flow velocity changes. Instead of a fixed control gain and phase, the controller will be a function of the flow velocity, which can be measured using a flow velocity sensor, attached upstream of the test model. In this case, the look-up table control method can be a potential method to be used to adjust the control gain and phase according to the optimal control performance at different flow velocities.

VI. CONCLUSIONS

The closed-loop control of flow-induced sound in a duct and the acoustic resonance inside downstream cavities was experimentally investigated. The main conclusions are summarized as follows.

(1) The closed-loop control method was developed by using a down-sampling method to utilize the high control actuation of THUNDER actuators. It was found that the flow-induced sound and the acoustic resonance inside the cavities, in particular, can be effectively reduced by the proposed closed-loop surface perturbation technique. Upon optimum tuning of the control parameters, a noise reduction of 17.5 and 22.6 dB was achieved in the duct and inside the cavity at the vortex shedding frequency, respectively.

(2) The closed-loop control could achieve a better control performance than that of the open-loop control. Based on the feedback response measured by a hot wire sensor, closed-loop control allows adjusting and optimizing the phase delay of control actuation so that the strength of vortex shedding energy could be minimized, leading to a larger level of noise reduction in the duct and cavity. This process was evident from the spectrum phase shift results for the closed-loop control case, where the vortex traveling time has been delayed downstream of the test model.

(3) The vortex shedding frequency shift phenomenon was observed in the closed-loop control. This phenomenon allowed more noise reduction inside the cavity than in the duct. The mechanism for the vortex shedding frequency shift in the closed-loop control is consistent with open-loop control. As such, the frequency shift can be predicted based on the proposed formula given in Eq. (4). As observed from the closed-loop control experiment, the frequency shift phenomenon led to a further sound pressure reduction of about 5.1 dB inside the acoustic cavity, compared to that in the duct.

(4) Two closed-loop control mechanisms for flow-induced sound were demonstrated in this work. (a) The impairment

of vortex shedding strength downstream of the test model: this is directly responsible for the sound reduction in the flow duct on the one hand and influences the correlated sound fields in the duct and inside the cavity on the other. (b) The shift of vortex shedding frequency that allows an additional noise reduction of acoustic resonance, particularly when the shedding frequency shift exceeds the resonance half-bandwidth for lightly damped resonant cavities.

ACKNOWLEDGMENT

The authors wish to acknowledge support given to them by the Research Grants Council of HKSAR through Grant No. PolyU 5132/07 E.

[1]J. H. Gerrard, "The mechanics of the formation region of vortices behind bluff bodies," J. Fluid Mech. **25**, 401–413 (1966).
[2]P. M. Radavich, A. Selamet, and J. M. Novak, "A computational approach for flow-acoustic coupling in closed side branches," J. Acoust. Soc. Am. **109**, 1343–1353 (2001).
[3]N. B. Roozen, M. Bockholts, V. E. Pascal, and A. Hirschberg, "Vortex sound in bass-reflex ports of loudspeakers. Part I. Observation of response to harmonic excitation and remedial measures," J. Acoust. Soc. Am. **104**, 1914–1918 (1998).
[4]L. Cattafesta, D. Williams, C. Rowley, and F. Alvi, "Review of active control of flow-induced cavity resonance," Report No. AIAA2003-3567.
[5]W. C. L. Shih, C. Wang, D. Coles, and A. Roshko, "Experiments on flow past rough circular cylinders at large Reynolds numbers," J. Wind Ind. Aerodyn. Eng. **49**, 351–368 (1993).
[6]E. Anderson and A. Szewczyk, "Effects of a splitter plate on the near wake of a circular cylinder in 2 and 3-dimensional flow configurations," Exp. Fluids **23**, 161–174 (1997).
[7]C. Dalton, Y. Xu, and J. C. Owen, "The suppression of lift on a circular cylinder due to vortex shedding at moderate Reynolds numbers," J. Fluids Struct. **15**, 617–628 (2001).
[8]S. Baek and H. J. Sung, "Numerical simulation of the flow behind a rotary oscillating circular cylinder," Phys. Fluids **10**, 869–876 (1998).
[9]S. Choi, H. Choi, and S. Kang, "Characteristics of flow over a rotationally oscillating cylinder at low Reynolds number," Phys. Fluids **14**, 2767–2777 (2002).
[10]O. Cetiner and D. Rockwell, "Streamwise oscillations of a cylinder in a steady current. Part 1: locked-on states of vortex formation and loading," J. Fluid Mech. **427**, 1–28 (2001).
[11]H. Blackburn and R. Henderson, "A study of two-dimensional flow past an oscillating cylinder," J. Fluid Mech. **385**, 255–286 (1999).
[12]E. Berger, "Suppression of vortex shedding and turbulence behind oscillating cylinders," Phys. Fluids **10**, 191–193 (1967).
[13]X. Y. Huang and D. S. Weaver, "On the active control of shear layer oscillations across a cavity in the presence of pipeline acoustic resonance," J. Fluids Struct. **5**, 207–219 (1991).
[14]L. N. Cattafesta III, S. Garg, M. Choudhari, and F. Li, "Active control of flow-induced cavity resonance," Report No. AIAA-97-1804.
[15]L. N. Cattafesta III, S. Garg and D. Shukla, "The development of piezoelectric actuators for active flow control," AIAA J. **39**, 1562–1568 (2001).
[16]L. N. Cattafesta III, J. Mathew, and A. Kurdila, "Modeling and design of piezoelectric actuators for fluid flow control," SAE 2000 Tran. J. Aero **109**, 1088–1095 (2001).
[17]S. Ziada, "Interaction of a jet-slot oscillator with a deep cavity resonator and its control," J. Fluids Struct. **15**, 831–843 (2001).
[18]S. Ziada, H. Ng, and C. Blake, "Flow-excited resonance of a confined shallow cavity in low Mach number flow and its control," J. Fluids Struct. **18**, 79–92 (2003).
[19]L. Cheng, Y. Zhou, and M. M. Zhang, "Perturbed interaction between vortex shedding and induced vibration," J. Fluids Struct. **17**, 887–901 (2003).
[20]M. M. Zhang, L. Cheng, and Y. Zhou, "Closed-loop-controlled vortex shedding from a flexibly supported square cylinder under different schemes," Phys. Fluids **16**, 1439–1448 (2004).
[21]L. Cheng, Y. Zhou, and M. M. Zhang, "Controlled flow-induced vibration on a fix-supported flexible cylinder in cross flow," J. Sound Vib. **292**, 279–299 (2006).
[22]M. M. Zhang, L. Cheng, and Y. Zhou, "Closed-loop controlled vortex-airfoil interactions," Phys. Fluids **18**(4), 046102 (2006).
[23]M. M. Zhang, L. Cheng, and Y. Zhou, "Control of post-stall airfoil aerodynamics based on surface perturbation," AIAA J. **46**, 2510–2519 (2008).
[24]J. P. Marouzé and L. Cheng, "A feasibility study of active vibration isolation THUNDER actuators," Smart Mater. Struct. **11**, 854–862 (2002).
[25]M. M. Zhang, L. Cheng, and Y. Zhou, "Asynchronous control of flow-induced acoustic cavity resonance using imbedded piezo-electric actuators," J. Acoust. Soc. Am. **126**(1), 36–45 (2009).
[26]Z. B. Lu and L. Cheng, "Active control of flow-induced acoustic resonance through surface perturbation," AIAA J. **50**(11), 2566–2573 (2012).
[27]S. Ziada and S. Shine, "Strouhal numbers of flow-excited acoustic resonance of closed side branches," J. Fluids Struct. **13**, 127–142 (1999).
[28]M. C. Welsh, A. N. Stokes, and R. Parker, "Flow-resonant sound interaction in a duct containing a plate, Part I: Semi-circular leading edge," J. Sound Vib. **95**(3), 305–323 (1984).
[29]R. J. Marks II, *Introduction to Shannon Sampling and Interpolation Theory* (Spinger-Verlag, New York, 1991), pp. 56–102.
[30]C. E. Shannon, "Communication in the presence of noise," in *Proceedings of the Institute of Radio Engineers* (January 1949), Vol. 37, No. 1, pp. 10–21.